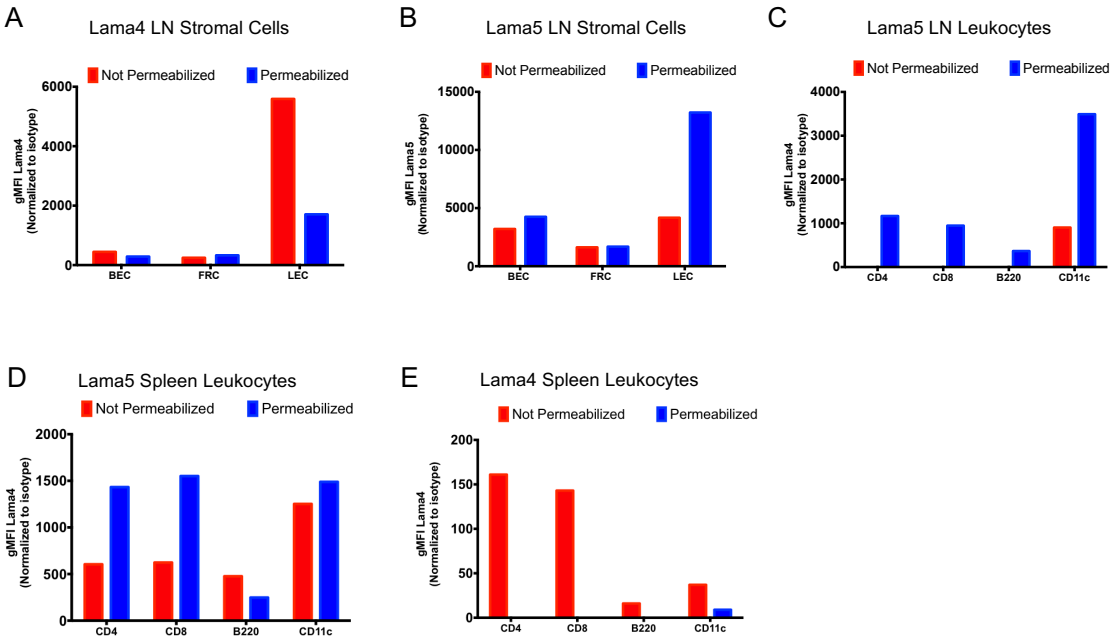

Figure S1. Expression of Lama4 and Lama5. Indicated cell subsets from C57BL/6 mouse LN and spleen analyzed by flow cytometry.

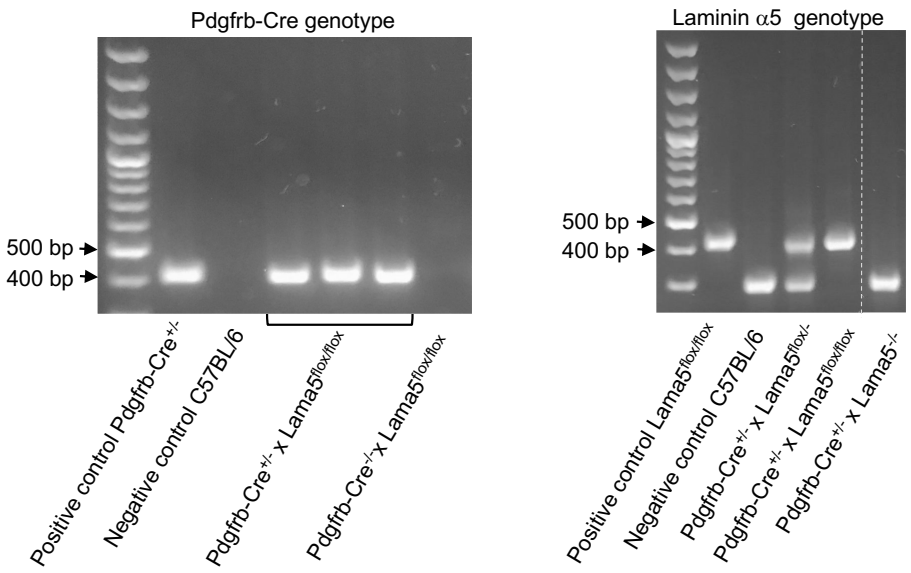

Figure S2. Genotypes of Lama5-flox and Pdgfrb-Cre mice. DNA sequences confirmed by genotyping Pdgfrb-Cre$^{+/-}$ x Lama5$^{flox/flox}$ (Cre$^{+/-}$) mice. The right portion of the vertical line in the second image is noncontiguous lane in the same gel.

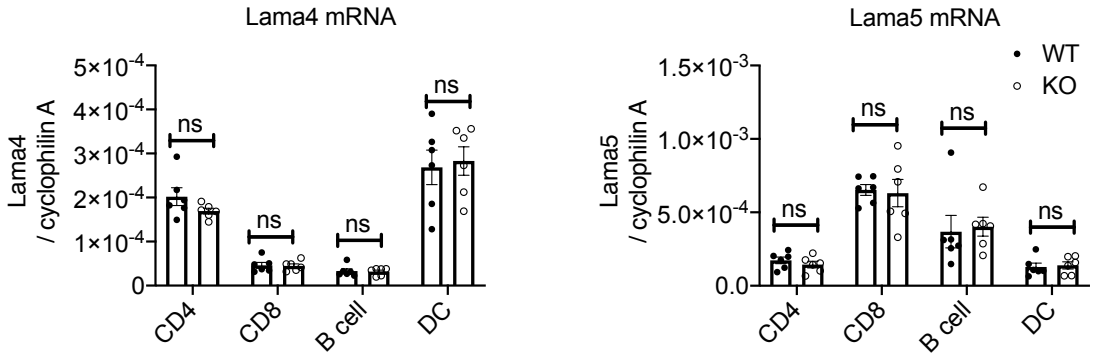

Figure S3. Lama4 and α5 mRNA in CD4, CD8 T cells, B cells and DC. Lama4 and Lama5 transcripts relative to cyclophilin A measured by qRT-PCR in the indicated cell subsets.

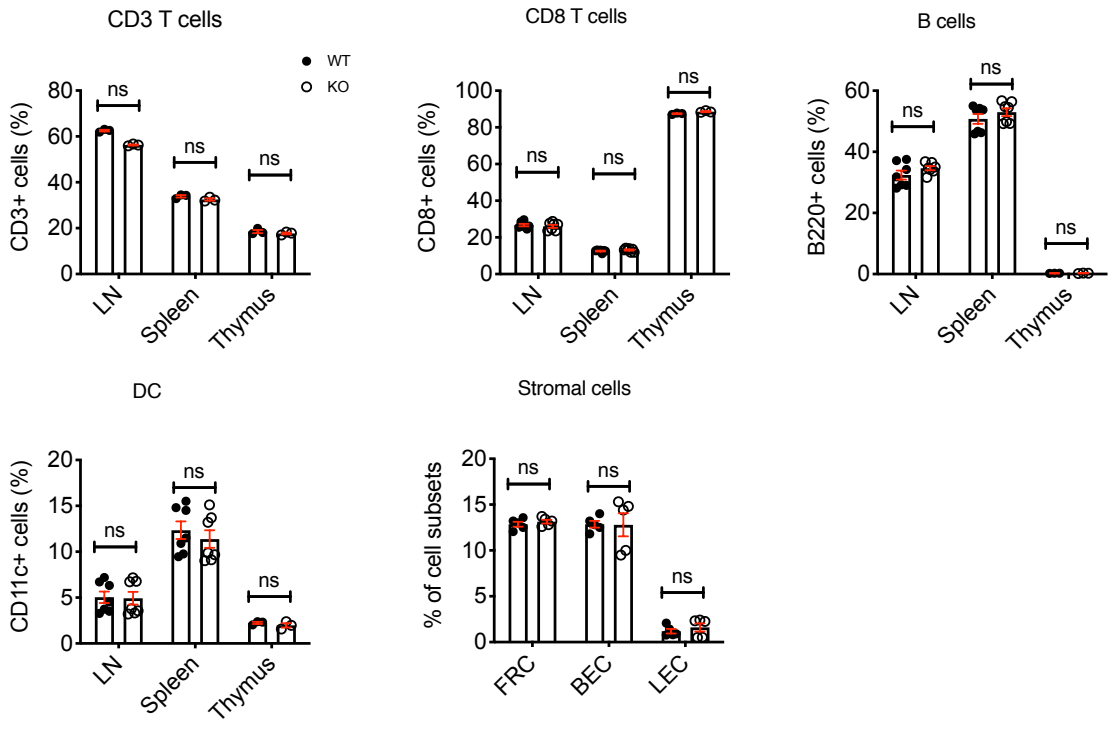

Figure S4. Depletion of LN stromal Lama5 does not affect T, B, DC and stromal cell numbers. Percentage of CD3 T cells, CD8 T cells, B cells, and DC in LN, spleens and thymus; and stromal cell subsets FRC, BEC and LEC in LN from Lama5 KO and WT mice analyzed by flow cytometry.

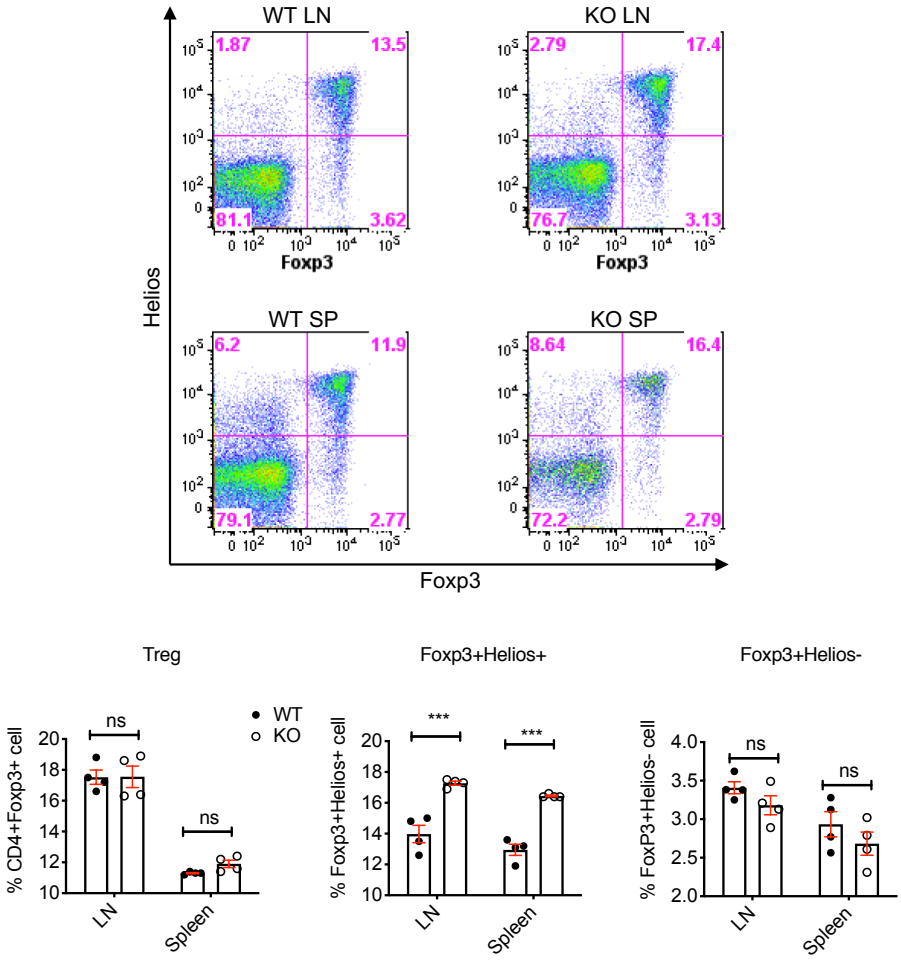

Figure S5. Depletion of LN stromal Lama5 does not alter the total numbers of Foxp3+ cells. LN and spleen cells from Lama5 KO and WT mice stained for CD4, Foxp3, and Helios and analyzed by flow cytometry. Student's unpaired 2-tailed t test. Mean ± SEM, *p < 0.05, **p < 0.01, ***p < 0.001.

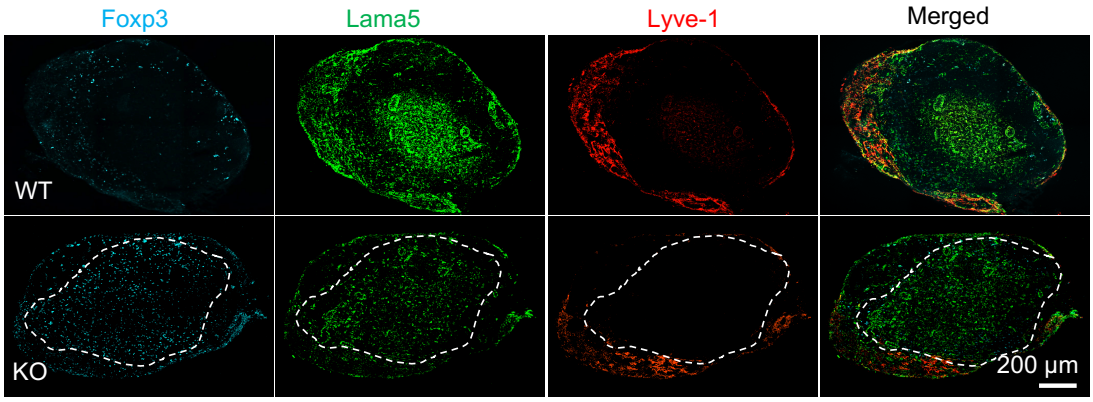

Figure S6: **Depleting stromal Lama5 increases Foxp3+ cells in paracortex, but not in subcapsular sinus.** Peripheral LN from Lama5 KO and WT mice stained for Foxp3, Lama5, and Lyve-1.

A

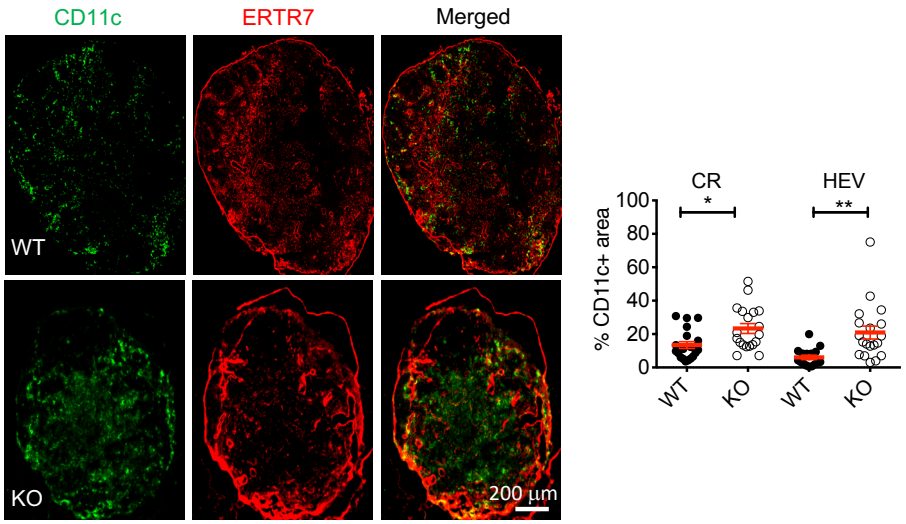

B

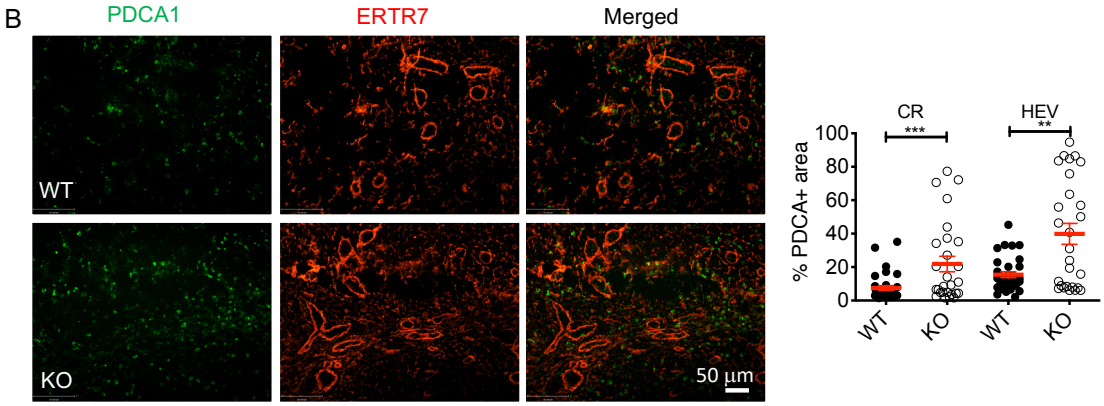

Figure S7: **Depleting stromal Lama5 increases CD11c DC in HEV.** LN from Lama5 KO and WT mice stained for CD11c (A) or PDCA1 (B) and ERTR7. Percentage of CD11c or PDCA1 positive areas quantified. Three independent experiments with 3 mice/group, 3 LN/mouse, 3 sections/LN and 3-5 fields/section. Student's unpaired 2-tailed t test. Mean ± SEM, *p < 0.05, **p < 0.01, ***p < 0.001.

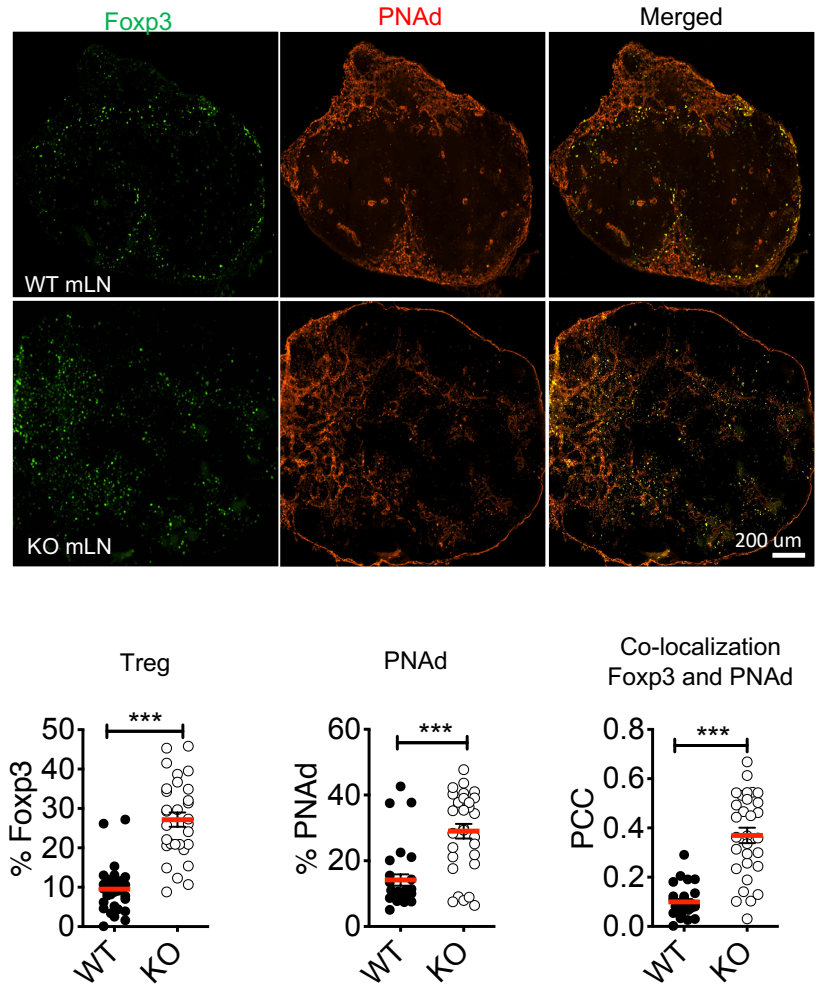

Figure S8: **Depleting stromal Lama5 increases Treg and HEV in mLN.** mLN from Lama5 KO and WT mice stained for Foxp3 and PNAd. Percentage of Foxp3 and PNAd positive areas quantified, and the co-localization between Foxp3 and PNAd analyzed with Pearson's correlation coefficient (PCC). Three independent experiments with 3 mice/group, 3 LN/mouse, 3 sections/LN and 3-5 fields/section. Student's unpaired 2-tailed t test. Mean ± SEM, *p < 0.05, **p < 0.01, ***p < 0.001.

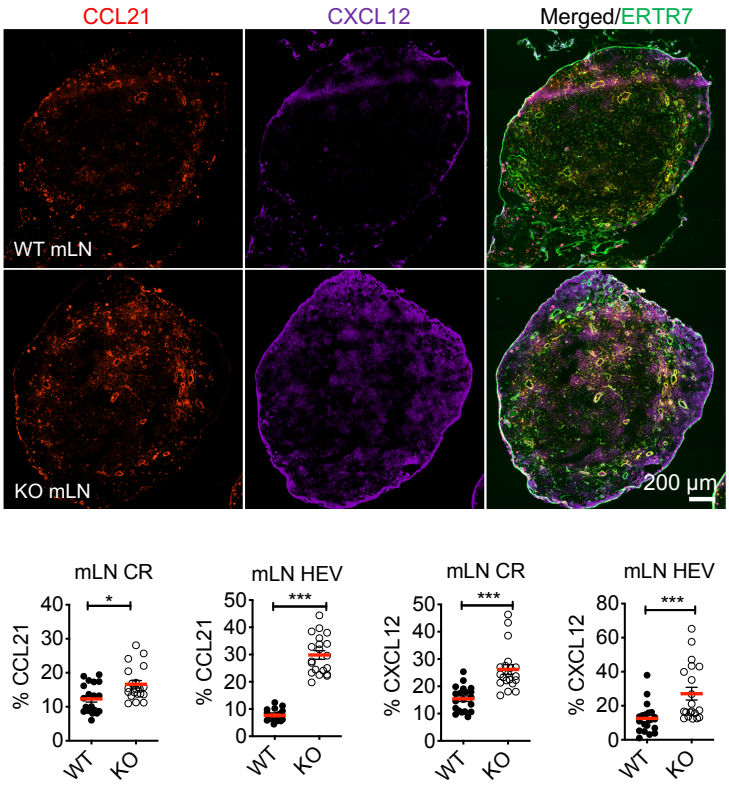

Figure S9: **Depleting stromal Lama5 increases CCL21 and CXCL12 in mLN.** mLN isolated from Lama5 KO and WT mice and stained for CCL21 and CXCL12. Percentages of CCL21 and CXCL12 positive areas in HEV and CR. Three independent experiments with 3 mice/group, 3 LN/mouse, 3 sections/LN and 3-5 fields/section. Student's unpaired 2-tailed t test. Mean ± SEM, *p < 0.05, **p < 0.01, ***p < 0.001.

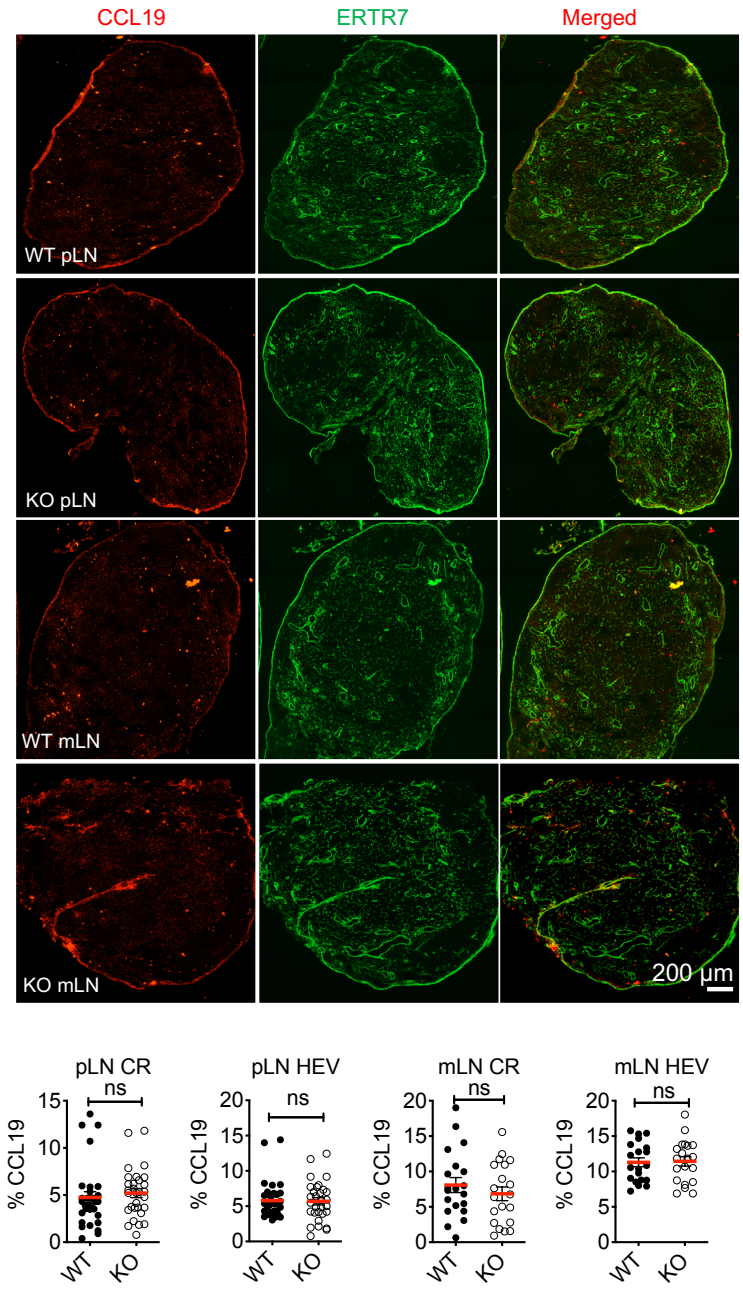

Figure S10. Depleting stromal Lama5 does not affect CCL19 in LN. pLN and mLN from KO and WT mice and stained for CCL19 and ERTR7. Percentages of CCL19 positive areas in HEV and CR quantified. Three independent experiments with 3 mice/group, 3 LN/mouse, 3 sections/LN and 3-5 fields/section. Student's unpaired 2-tailed t test. Mean ± SEM, *p < 0.05, **p < 0.01, ***p < 0.001.

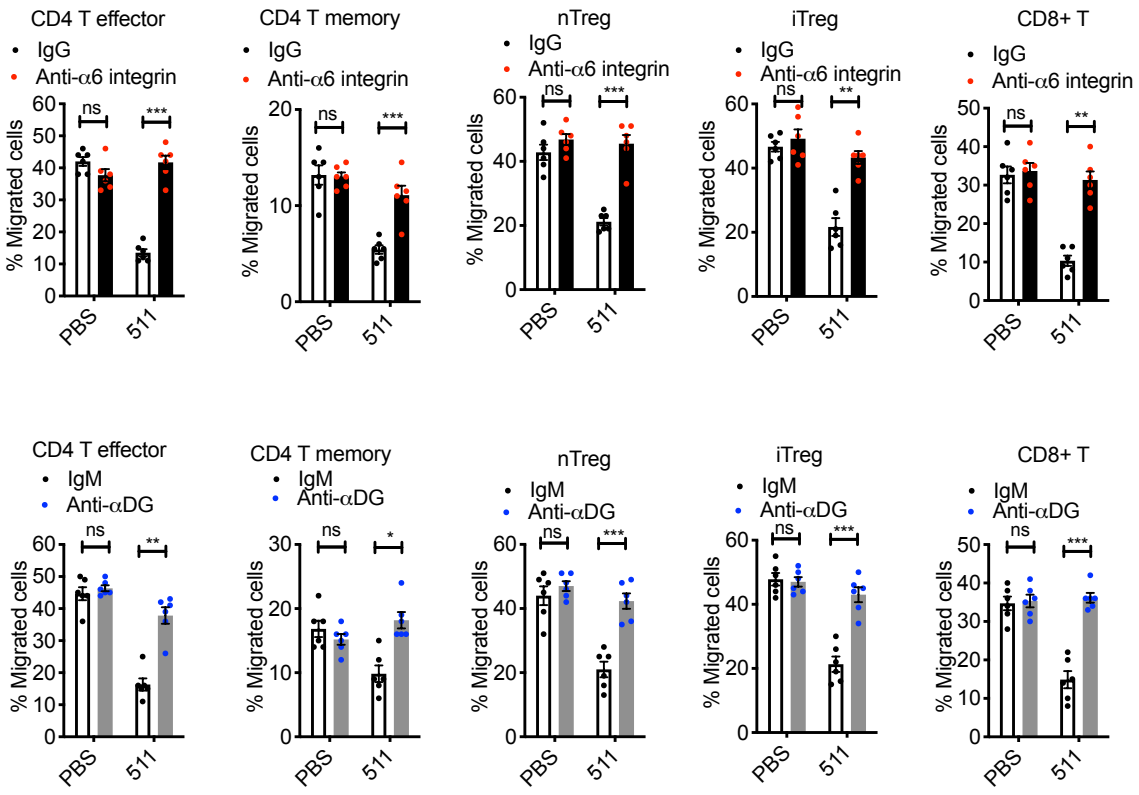

Figure S11. Lama5 inhibits TEM of various T cell subsets by α6-integrin and αDG. A-B Anti-α6 integrin or anti-αDG pretreatment of CD4 T effector and memory cells, natural and induced Treg, and CD8 T cells to block laminin 511 receptors. Percentage of migrated cells. Mean ± SEM of 3 independent experiments. *p < 0.05, **p < 0.01, ***p < 0.001, by one-way ANOVA.

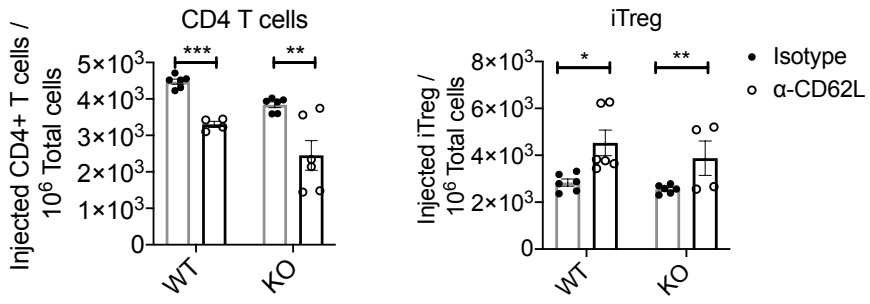

Figure S12. Depleting stromal Lama5 does not enhance T cell retention. A mixture of 2 x 10^6 eFlour670+ CD4 T cells and 2 x 10^6 CFSE+ Treg injected i.v. into Lama5 KO mice or littermate controls. After 18h, 100 μg anti-CD62L or control Rat IgG2a injected. 18h after antibody injection, the remaining eFlour670+ CD4 T cells and CFSE+ iTreg in LN measured by flow cytometry. Data presented as cell numbers out of 10^6 total cells. 3 mice/group, 5 LN/mouse Mean ± SEM, *p < 0.05, **p < 0.01, ***p < 0.001.

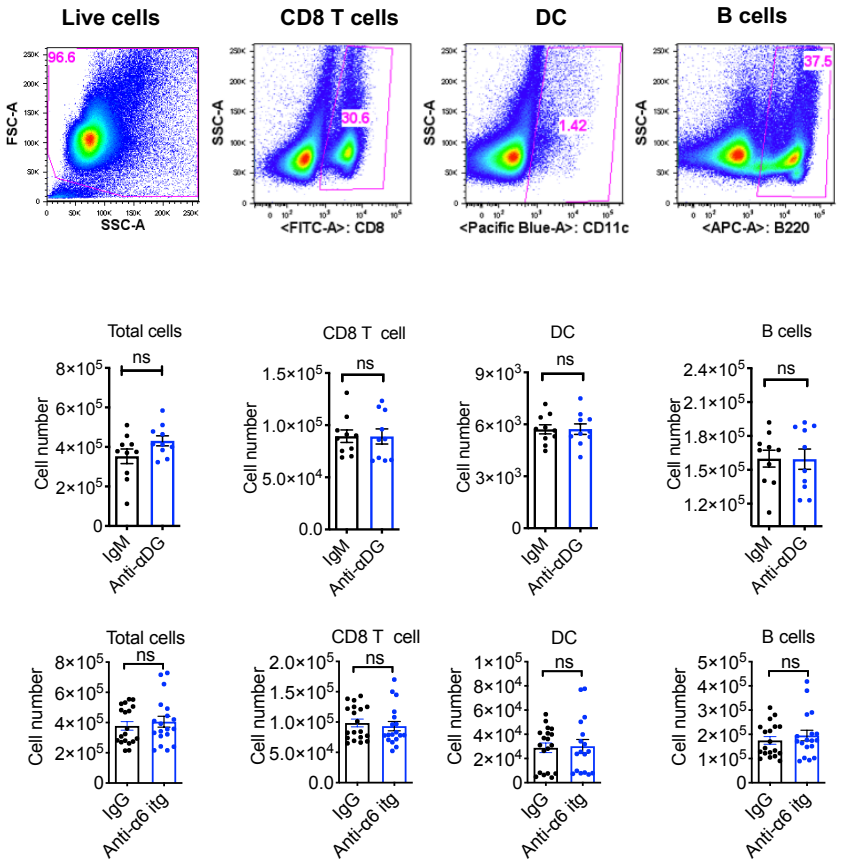

Figure S13. Blockage of αDG or α6 integrin does not alter the numbers of total, CD8 T, DC or B cells in LN. C57BL/6 mice injected i.v. with 10 μg anti-α-DG mAb (isotype IgM), or 10 μg anti-α6 integrin (isotype IgG), and 16 hours later LN harvested and single cells stained for CD8, CD11c, and B220. Total cell numbers and each subset counted by flow cytometry. Upper panels: gating strategy. Lower panels: total cells, CD8+ T cells, DCs, and B cells in each LN. Three independent experiments, 2 mice/group, 5 LN/mouse. Student's unpaired 2-tailed t test. Mean ± SEM, *p < 0.05, **p < 0.01, ***p < 0.001.

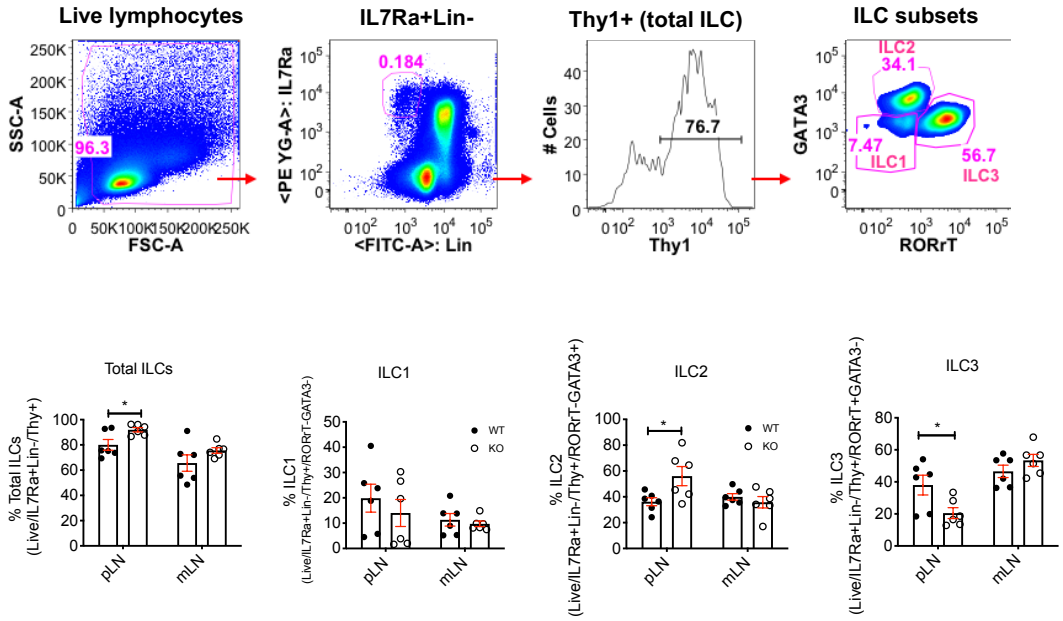

Figure S14. Depletion of LN stromal Lama5 increases type 2 innate lymphoid cells (ILC2). Upper panel, gating strategy. Bottom panel, ILC subsets in LNs.

Supplementary Table 1: Antibodies used for flow and immunohistochemistry

Antibodies	Host	Clone	Application	Vendor
Anti-CD3ε	Rabbit	145-2C11	activation	eBioscience
Anti-CD28	Syrian hamster	37.51	IHC	eBioscience
Anti-CD3	Rabbit	Polyclonal	IHC	abcam
Anti-CD4	Rat	GK1.5	FACS	Biolegend
Anti-Lama4	Rat	775830	IHC	R&D
Anti-Lama5	Rabbit	Polyclonal	IHC	Novus Biological
Anti-PNAd	Rat	MECA-79	IHC	BD Biosciences
Anti-ER-TR7	Rat	sc-73355	IHC	Santa Cruz
Anti-Rabbit IgG	Goat	Polyclonal	IHC	Jackson Immunoresearch
Anti-Rat IgG	Goat	Polyclonal	IHC	Jackson Immunoresearch
Anti-Rabbit IgG	Donkey	Polyclonal	IHC	Jackson Immunoresearch
Anti-Rat IgM	Goat	Polyclonal	IHC	Jackson Immunoresearch
Alexa Fluor 405 Anti-Rabbit	Donkey	Polyclonal	IHC	Jackson Immunoresearch
Alexa Fluor 488 Anti-rat	Donkey	Polyclonal	IHC	Jackson Immunoresearch
Alexa Fluor 568 Anti-Goat	Donkey	Polyclonal	IHC	Jackson Immunoresearch
Alexa Fluor 647 Anti-rabbit	Donkey	Polyclonal	IHC	Jackson Immunoresearch
Anti-CXCL9	Rabbit	11H1L14	IHC	Invitrogen
Anti-CXCL10	Goat	Polyclonal	IHC	R&D
Anti-CXCL12	Rabbit	Polyclonal	IHC	Invitrogen
Anti-CXCL12	Mouse	#79018	FACS	R&D
Anti-CCL21	Rat	# 59106	FACS	R&D
Anti-CD31	Rabbit	Polyclonal	IHC	abcam
Anti-B220	Rat	RA3-6B2	FACS	eBioscience
Anti-FoxP3	Rat	NRRF-30	IHC	Invitrogen
Anti-CD11c	HL3	Armenian Hamster	IHC	BD Biosciences
Anti-Lyve1	Rat	ALY7	IHC	R&D systems
Anti-mouse-IL4	Rat	11B11	Inhibition	eBioscience
Anti-CD69-PE-Cy7	Armenian hamster	H1.2F3	FACS	eBioscience
Anti-CD25-PE	Rat	PC61.5	FACS	eBioscience

Anti-CD44-APC	Rat	IM7	FACS	eBioscience
Anti-Foxp3-APC	Rat	PCH101	FACS	Thermofisher Scientific
Anti-α6 integrin	Rat	GoH3	Inhibition	Biolegend
anti-α-dystroglycan	Rabbit	IIH6C4	Inhibition	MilliporeSigma
Anti-CD40L	Armenian Hamster	MR-1	Inhibition	Bio X Cell
Anti-CD62L	Rat	MEL-14	Inhibition	BioXcell

Supplementary video 1: T cell motility on PBS coated plate surface. PBS coated on to 24 well plates, $5x10^5$ CD4 T cells seeded into each well, and migration recorded with real-time live imaging system. Images recorded at 1-minute intervals for 30 mins under EVOS microscope with 10X lens.

Supplementary video 2: T cell motility on Laminin 411 coated plate surface. 2 µg/ml laminin 411 coated on to 24 well plates, $5x10^5$ CD4 T cells seeded into each well, and migration recorded with real-time live imaging system. Images recorded at 1-minute intervals for 30 mins under EVOS microscope with 10X lens.

Supplementary video 3: T cell motility on Laminin 511 coated plate surface. 1 µg/ml laminin 511 coated on to 24 well plates, $5x10^5$ CD4 T cells seeded into each well, and migration recorded with real-time live imaging system. Images recorded at 1-minute intervals for 30 mins under EVOS microscope with 10X lens.

Supplementary video 4: T cell motility on Laminin 411+511 coated plate surface. 2 µg/ml laminin 411 and 1 µg/ml laminin 511 coated on to 24 well plates, $5x10^5$ CD4 T cells seeded into each well, and migration recorded with real-time live imaging system. Images recorded at 1-minute intervals for 30 mins under EVOS microscope with 10X lens.